

Published in final edited form as:

*J Mol Cell Cardiol.* 2010 February ; 48(2): 395. doi:10.1016/j.yjmcc.2009.10.004.

## Palmitate Attenuates Myocardial Contractility through Augmentation of Repolarizing Kv Currents

Todd E. Haim<sup>3,†</sup>, Wei Wang<sup>1,†</sup>, Thomas P. Flagg<sup>2,‡</sup>, Michael A. Tones<sup>3</sup>, Anthony Bahinski<sup>3</sup>, Randal E. Numann<sup>3</sup>, Colin G. Nichols<sup>2</sup>, and Jeanne M. Nerbonne<sup>1,\*</sup>

<sup>1</sup>Department of Developmental Biology, Washington University School of Medicine, St. Louis, MO 63110

<sup>2</sup>Department of Cell Biology and Physiology, Washington University School of Medicine, St. Louis, MO 63110

<sup>3</sup>Pfizer Global Research and Development, Chesterfield, MO, 63017

### Abstract

There is considerable evidence to support a role for lipotoxicity in the development of diabetic cardiomyopathy, although the molecular links between enhanced saturated fatty acid uptake/metabolism and impaired cardiac function are poorly understood. In the present study, the effects of acute exposure to the saturated fatty acid, palmitate, on myocardial contractility and excitability were examined directly. Exposure of isolated (adult mouse) ventricular myocytes to palmitate, complexed to bovine serum albumin (palmitate:BSA) as in blood, rapidly reduced (by 54±4%) mean (± SEM) unloaded fractional cell shortening. The amplitudes of intracellular Ca<sup>2+</sup> transients decreased in parallel. Current-clamp recordings revealed that exposure to palmitate:BSA markedly shortened action potential durations at 20, 50 and 90% repolarization. These effects were reversible and were occluded when the K<sup>+</sup> in the recording pipettes was replaced with Cs<sup>+</sup>, suggesting a direct effect on repolarizing K<sup>+</sup> currents. Indeed, voltage-clamp recordings revealed that palmitate:BSA reversibly and selectively increased peak outward voltage-gated K<sup>+</sup> (Kv) current amplitudes by 20 ± 2%, whereas inwardly rectifying K<sup>+</sup> (Kir) currents and voltage-gated Ca<sup>2+</sup> currents were unaffected. Further analyses revealed that the individual Kv current components I<sub>to,f</sub>, I<sub>K,slow</sub> and I<sub>ss</sub>, were all increased (by 12 ± 2 %, 37 ± 4 % and 34 ± 4, respectively) in cells exposed to palmitate:BSA. Consistent with effects on both components of I<sub>K,slow</sub> (I<sub>K,slow1</sub> and I<sub>K,slow2</sub>) the magnitude of the palmitate-induced increase was attenuated in ventricular myocytes isolated from animals in which the Kv1.5 (I<sub>K,slow1</sub>) or the Kv2.1 (I<sub>K,slow2</sub>) locus was disrupted and I<sub>K,slow1</sub> or I<sub>K,slow2</sub> is eliminated. Both the enhancement of I<sub>K,slow</sub> and the negative inotropic effect of palmitate:BSA were reduced in the presence of the Kv1.5 selective channel blocker, diphenyl phosphine oxide-1 (DPO-1). Taken together, these results suggest that elevations in circulating saturated free fatty acids, as occurs in diabetes, can directly augment repolarizing myocardial Kv currents and impair excitation-contraction coupling.

© 2009 Elsevier Ltd. All rights reserved.

\*To whom correspondence should be addressed: Jeanne M. Nerbonne, PhD, Department of Developmental Biology, Washington University School of Medicine, 660 S. Euclid Ave., Box 8103, St. Louis, MO 63110, Ph: (314) 362-2564, Fax: (314) 362-7463, jnerbonne@wustl.edu.

†These authors contributed equally to this work.

‡Present address: Department of Anatomy, Physiology and Genetics, Uniformed Services University of the Health Sciences, 4301 Jones Bridge Rd., C-2114, Bethesda, MD 20814

**Publisher's Disclaimer:** This is a PDF file of an unedited manuscript that has been accepted for publication. As a service to our customers we are providing this early version of the manuscript. The manuscript will undergo copyediting, typesetting, and review of the resulting proof before it is published in its final citable form. Please note that during the production process errors may be discovered which could affect the content, and all legal disclaimers that apply to the journal pertain.

## INTRODUCTION

Altered energy metabolism is a prominent feature of, and in some instances may cause, heart failure [1,2]. For example, cardiac dysfunction is a prominent feature of diabetes mellitus and it is clear that impaired cardiac function can occur in individuals with diabetes without evidence of any other secondary risk factors for heart disease, including hypertension or atherosclerosis, suggesting that the metabolic consequences of diabetes alone are sufficient to impair cardiac function [3,4]. These observations also suggest that derangements of cardiac metabolism can have direct consequences on cardiac function. The potential molecular mechanisms that link altered metabolism with cardiac pathology are numerous [2], although poorly understood.

In the normal heart, lipid oxidation accounts for about 60% of the total ATP generated, while glycolysis supplies the remainder [5,6]. In the diabetic heart, in contrast, 80–90% of the ATP is generated from lipid oxidation as a direct result of increased circulating free fatty acids and reduced insulin sensitivity [7–9]. In previous studies, we demonstrated that transgenic mice (MHC-FATP) overexpressing fatty acid transport protein 1 (FATP-1) specifically in the myocardium exhibit increased myocardial lipid uptake, storage and metabolism [10]. In addition, MHC-FATP mice have impaired diastolic function [10,11], one of the earliest signs of diabetic cardiomyopathy [12,13]. These findings support the hypothesis that altered cardiac metabolism alone is sufficient to impair cardiac function.

Importantly, however, the later stages of diabetic cardiomyopathy in humans are also characterized by impaired systolic function [14–16]. In addition, marked systolic dysfunction has been observed in several animal models of diabetes, including streptozotocin-induced diabetes in rats and mice, Zucker diabetic fatty rats and in *db/db* mice [9,17–19]. In contrast to the MHC-FATP transgenic mice in which the metabolic derangements are restricted to the myocardium [10], these animal models of diabetes exhibit systemic metabolic abnormalities, including increases in circulating saturated fatty acids [9,20]. The phenotypic differences between these models and the MHC-FATP mice also indicate that altered substrate usage in the heart alone is insufficient to explain the observed systolic dysfunction [10,11], further suggesting that the systemic increases in circulating free fatty acids that are associated with diabetes [19,21] might contribute directly to systolic dysfunction.

The experiments here were designed to explore directly the functional consequences of acute exposure to palmitate, complexed with bovine serum albumin (BSA) as in blood, on the mechanical and electrical properties of isolated (adult mouse) ventricular myocytes. Consistent with the notion that elevated circulating fatty acids may contribute to systolic dysfunction in cardiac disease, these experiments demonstrate reversible inhibition of unloaded cell shortening in response to elevated palmitate. In addition, the results of further electrophysiological experiments suggest that the negative inotropic effect of palmitate:BSA is due to shortening of action potential durations, resulting from palmitate-induced augmentation of repolarizing voltage-gated  $K^+$  ( $K_v$ ) currents.

## Materials and Methods

### Animals

Adult wild type (WT), SWAP [22], and  $Kv2.1^{-/-}$  (Deltagen Corporation) C57BL6 mice were used in the experiments here. All animals were handled in accordance with the NIH Guide for the Care and Use of Laboratory Animals, and all protocols were approved by the Washington University Animal Studies Committee.

## Isolation of Adult Mouse Ventricular Myocytes

Myocytes were isolated from the left ventricles of adult (8–12 week) WT, SWAP or Kv2.1<sup>-/-</sup> C57BL6 mice using enzymatic and mechanical methods that have been described previously in detail [23,24]. Following dispersion, isolated left ventricular myocytes were stored in isolation medium containing (in mM): NaCl, 116 mM; KCl, 5.3 mM; CaCl<sub>2</sub>, 0.15 mM; NaH<sub>2</sub>PO<sub>4</sub>, 1.2 mM; glucose, 11.6 mM; MgCl<sub>2</sub>, 3.7 mM; HEPES, 20 mM; L-glutamine, 2.0 mM; NaHCO<sub>3</sub>, 4.4 mM; KH<sub>2</sub>PO<sub>4</sub>, 1.5 mM; and supplemented with 1x essential vitamins and amino acids (GIBCO) at room temperature. Cells were used in experiments within 12 hr of isolation.

## Solutions

For experiments, palmitate (Nu-Chek Prep # N-16-A) was complexed with fatty acid free bovine serum albumin (BSA, Sigma #A-6003). Stock solutions containing 20% BSA were prepared in sterile phosphate buffered saline (PBS) and stored at 4°C. Complexed palmitate:BSA solutions were then prepared by mixing aliquots of 20 mM palmitic acid (prepared fresh in sterile H<sub>2</sub>O) and the 20% fatty acid free BSA stock solution at a 1:2 molar ratio in normal Tyrode solution. The resulting solutions were sterile filtered and stored at 4°C (for up to one week) for use in experiments. The palmitate concentrations provided in the text represent the total (not the calculated free) palmitate concentrations in the solutions. The calculated free palmitate concentration, using the method of Richieri and colleagues [25], with a palmitate:BSA ratio of 1:2 was 42 nM. This final unbound palmitate concentration (of 42 nM) was selected based on previous reports that this concentration would not cause “lipotoxicity” [26]. This concentration is, however, expected to be in the low pathological range of unbound free fatty acid concentrations, reported to be as high as 100 nM [27].

## Cell Contractility and Calcium Transient Measurements

Unloaded cell shortening and calcium transients were measured in isolated adult mouse left ventricular myocytes. For experiments, isolated left ventricular cells were transferred to a recording chamber mounted on the stage of a Nikon Diaphot inverted microscope and perfused with normal Tyrode solution containing (in mM): NaCl, 137; KCl, 5.4; NaH<sub>2</sub>PO<sub>4</sub>, 0.16; glucose, 10; CaCl<sub>2</sub>, 1.8; MgCl<sub>2</sub>, 0.5; HEPES, 5.0; NaHCO<sub>3</sub>, 3.0; pH 7.3–7.4). All experiments were performed at room temperature. Video images of individual myocyte contractions were acquired and analyzed using a Myocam camera (IonOptix).

To determine the effect of acute palmitate applications on contractility, isolated myocytes were transferred to the recording chamber, field stimulated (20 V @ 1 Hz) and superfused with normal Tyrode solution. After 30 seconds of recording in control solution, the superfusion solution was changed (using a rapid solution switcher; Warner Instruments) to Tyrode containing 75 μM palmitate:150 μM BSA (or the indicated concentrations of palmitate and BSA). At each solution change, contraction parameters were re-measured after 5 minutes of continuous superfusion or earlier when a new steady state contraction was clearly reached prior to this (5 min) time point. This was often the case when the highest concentration of palmitate:BSA (75 μM) was applied (e.g. Figure 1A). To assess the effects of the Kv channel blocker, Diphosphine Oxide 1 (DPO-1, Tocris Bioscience)[28], a similar experimental strategy, involving switching the superfusion solution during continuous field stimulation. Following 30 seconds of baseline recording, the solution was switched to Tyrode containing 1 μM DPO-1 and 6 superfused for 5 minutes or until a new baseline was achieved. The superfusion solution was then switched to Tyrode containing 1 μM DPO-1 and 75 μM palmitate/150 μM BSA, followed by Tyrode lacking DPO-1, i.e., containing 75 μM palmitate/150 μM BSA alone; washout was obtained by superfusion of normal Tyrode solution.

In experiments focused on measuring intracellular free  $\text{Ca}^{2+}$  concentrations  $[\text{Ca}^{2+}]_i$ , isolated ventricular myocytes were incubated in isolation medium (see above) containing (0.5 – 1  $\mu\text{M}$ ) fluo-4-AM (Molecular Probes, Inc.) and (0.02%) pluronic acid (Sigma) for 30–60 minutes at room temperature. Following washing with fresh isolation medium, fluo-loaded myocytes were transferred to the recording chamber and superfused with normal Tyrode solution supplemented with 500  $\mu\text{M}$  probenecid (Sigma) to inhibit dye export [29]. Myocytes were then field stimulated and the superfusion solution was changed as described above. Emitted fluorescence was captured with a photomultiplier tube (IonOptix).

### Electrophysiological Recordings

Whole-cell current- and voltage-clamp recordings were obtained from myocytes isolated from the left ventricular apex (LVA) of adult mouse hearts. Current- and voltage-clamp recordings were obtained from cells within 12 hr of isolation using a Dagan 3900A (Dagan Corporation) whole-cell patch clamp amplifier, interfaced to a Digidata 1332A A/D converter (Molecular Devices) with the pClamp (version 9.2, Molecular Devices) software package. For action potential recording, the bath solution contained (in mM): 136 NaCl, 4 KCl, 2  $\text{MgCl}_2$ , 1  $\text{CaCl}_2$ , 10 HEPES and 10 glucose (pH 7.4; 300 mOsm). For recordings of voltage-gated  $\text{K}^+$  ( $\text{K}_v$ ) currents, clamp experiments, the bath solution also contained 20  $\mu\text{M}$  Tetrodotoxin (TTX) and 0.5 mM  $\text{CdCl}_2$  to block voltage-gated  $\text{Na}^+$  and  $\text{Ca}^{2+}$  currents, respectively. Recording pipettes routinely contained (in mM): 135 KCl, 5  $\text{K}_2\text{ATP}$ , 10 EGTA, 10 HEPES and 5 glucose (pH 7.2; 310 mOsm). In some experiments,  $\text{Cs}^+$  and tetraethylammonium (TEA) were used (in place of the  $\text{K}^+$ ) in the recording pipettes to block outward  $\text{K}^+$  currents; in this case, the pipette solution contained (in mM): 15 NaCl, 100 CsCl, 30 TEA-Cl, 5  $\text{MgATP}$ , 10 EGTA, 10 HEPES and 5 glucose (pH 7.2; 310 mOsm). Pipette resistances were 1.5–3  $\text{M}\Omega$  when filled with either recording solution.

After formation of a giga-seal ( $>1\text{G}\Omega$ ), the whole-cell configuration was established and whole-cell membrane capacitances ( $C_m$ ) and input resistances were measured in each cell in response to brief  $\pm 10\text{mV}$  voltage steps from a holding potential (HP) of  $-70\text{mV}$ .  $C_m$  and series resistances were electronically compensated by  $\sim 85\%$ . Current amplitudes were always  $<10\text{nA}$  and voltage errors resulting from the uncompensated series resistances were always  $<9\text{mV}$  and were not corrected. Leak currents were  $<50\text{pA}$  and were also not corrected. Data were acquired at 10 or 100 KHz and signals were low-pass filtered at 5 kHz before digitization and storage.

In the current-clamp mode, action potentials were evoked by brief (4 ms) current ( $\sim 800\text{pA}$ ) injections at 15 s intervals. In the voltage-clamp experiments, depolarization-activated outward  $\text{K}^+$  ( $\text{K}_v$ ) currents, evoked in response to 4.5 s voltage steps to test potentials between  $-60$  and  $+40\text{mV}$  from a holding potential (HP) of  $-70\text{mV}$ , were recorded; voltage steps were presented in 10 mV increments at 15 s intervals. In experiments focused on determining the time-course of palmitate-mediated effects,  $\text{K}_v$  currents, evoked in response to 4.5s depolarizing voltage steps to  $+40\text{mV}$  from the HP of  $-70\text{mV}$ , presented at 15 s intervals, were recorded. Inwardly rectifying  $\text{K}^+$  currents ( $\text{I}_{\text{K}1}$ ), evoked during 4.5 s voltage steps to test potentials between  $-90$  and  $-120\text{mV}$  from the same HP, were also recorded in some experiments.

A manual multimanifold superfusion system was used to apply the palmitate:BSA and DPO-1 ( $\text{K}^+$  channel blocker) containing solutions to single myocytes during electrophysiological recordings. Solutions were superfused at  $\sim 0.2\text{ml/min}$  and the distance between the tip of the superfusion pipette (ID: 0.008") and the cell was kept to an absolute minimum to ensure that the onset and offset of each application was rapid and that the applications were local and constant.

## Data Analyses

Intracellular  $\text{Ca}^{2+}$  measurements were analyzed using IonWizard, Clampfit, GraphPad, and Microsoft Excel and results are presented as means  $\pm$  SEM (standard error of the means). The statistical significance of differences between groups was assessed using the Student's *t* test and *P* values are presented in the text and in the Figures; *n* values provided represent the numbers of cells examined.

Electrophysiological data were compiled and analyzed using *Clampfit* 9.2 (Axon Instruments) and *GraphPad* (Prism) software. Integration of the capacitative transients recorded during brief  $\pm 10$  mV voltage steps from the HP ( $-70$  mV) allowed determination of whole-cell membrane capacitances ( $C_m$ ). Current amplitudes were normalized to the cell capacitance and currents densities (pA/pF) are reported. Resting membrane potentials ( $V_m$ ), action potential amplitudes (APA), and action potential durations at 20% (APD<sub>20</sub>), 50% (APD<sub>50</sub>) and 90% (APD<sub>90</sub>) repolarization were measured directly from the action potential waveforms using *Clampfit* 9.2. Peak  $\text{K}_v$  currents at each test potential ( $I_{\text{peak}}$ ) were defined as the maximal outward  $\text{K}_v$  currents recorded during the 4.5 s voltage steps. Steady-state outward  $\text{K}_v$  currents ( $I_{\text{ss}}$ ) were measured directly as the currents remaining at the end of 4.5s voltage steps. The decay phases of the outward  $\text{K}_v$  currents recorded during the 4.5s voltage steps were also fitted by a biexponential function ( $y(t) = A1(\exp(-t/\tau1) + A2(\exp(-t/\tau2) + B)$ ) to provide the amplitudes of  $I_{\text{to,f}}$ ,  $I_{\text{K,slow}}$  and  $I_{\text{ss}}$  and the time constants of  $I_{\text{to,f}}$  and  $I_{\text{K,slow}}$  decay [23,30].  $I_{\text{K1}}$  amplitudes at  $-120$  mV were measured at the peak of the inward currents. The  $\text{IC}_{50}$  and Hill coefficients ( $n_{\text{H}}$ ) for DPO-1-mediated effects on  $\text{K}_v$  currents were obtained from fits of the normalized current amplitudes, plotted as a function of the log of the DPO-1 concentration  $[\text{DPO-1}] \text{ \%Change} = 1/[1 + ([\text{DPO-1}]/\text{IC}_{50})^{n_{\text{H}}}]$ , as described previously [28].

Electrophysiological data are also presented as means  $\pm$  S.E.M. Statistical differences in measured parameters were evaluated using paired (compared in the same cell) or unpaired (for comparisons of mean values) two-tailed Student's *t* test; *P* (presented in the text and Figures) values of  $<0.05$  were considered significant.

## RESULTS

### Palmitate Inhibits Ventricular Myocyte Contractility

Although it has been suggested that increases in circulating saturated fatty acids contribute to the development of diabetic cardiomyopathy [7,8], the effects of elevated free fatty acids on myocardial cell functioning have not been widely studied and remain poorly understood. To explore this question, the effects of acute exposure to palmitate on contractile function of field-stimulated, isolated wild-type (WT) adult mouse ventricular myocytes were assessed. Exposure to (75  $\mu\text{M}$ ) palmitate, complexed to (150  $\mu\text{M}$ ) BSA, as described in **Materials and Methods**, significantly ( $P < 0.001$ ) reduced unloaded fractional cell shortening in WT ventricular myocytes from a mean ( $\pm$  SEM;  $n = 28$ ) of  $7.8 \pm 0.9\%$  to  $3.6 \pm 0.4\%$  (Figure 1A and B). In contrast, BSA alone (150  $\mu\text{M}$ ) had no effect on cell contraction (Figure 1A). Steady-state unloaded cell shortening was also observed to vary as a function of the total fatty acid concentration (Figure 1D) in the superfusion solution, i.e., in solutions made by changing both the palmitate and BSA concentrations in parallel while maintaining a constant palmitate:BSA ratio of 1:2 (see **Discussion**).

Previous studies have demonstrated that prolonged (20 minute pre-incubation) exposures to palmitate also result in marked decreases in cell contractility and that this reflects decreased intracellular  $\text{Ca}^{2+}$  concentration [31]. To determine whether a similar mechanism underlies the negative inotropic effect of palmitate:BSA applied acutely, intracellular  $\text{Ca}^{2+}$  transients were examined in field stimulated myocytes loaded with the  $\text{Ca}^{2+}$ -indicator, Fluo-4 (see **Materials**

**and Methods**). Consistent with the observed effect on contraction (Figure 1), exposure to palmitate:BSA resulted in a rapid decrease in the amplitudes of intracellular  $\text{Ca}^{2+}$  transients (Figure 2), with no effect on the rates of rise or decay ( $\text{Ca}^{2+}$  removal) of the transients (Figure 2). Taken together, these results suggest that acute exposure to palmitate specifically attenuated myocardial contractility by reducing the intracellular  $\text{Ca}^{2+}$  transient, likely reflecting reduced  $\text{Ca}^{2+}$  influx and/or reduced release of  $\text{Ca}^{2+}$  from intracellular stores.

### Palmitate Reduces Sarcolemmal Excitability by Increasing Voltage-gated $\text{K}^+$ Currents

The rate of decline of the  $\text{Ca}^{2+}$  transients in WT mouse ventricular myocytes is largely dependent on the functioning of the sarcoplasmic reticulum ATPase, SERCA [32]. The lack of any measurable effects of palmitate:BSA on the kinetics of the ventricular  $\text{Ca}^{2+}$  transients in the experiments described above (Figure 2), therefore, suggests that the functioning of the sarcoplasmic reticulum is not measurably affected by acute exposures to elevated palmitate:BSA. In addition, these observations further suggested that palmitate:BSA may affect sarcolemmal membrane excitability. To examine this possibility directly, whole-cell action potentials were measured in myocytes isolated from the left ventricular apex (LVA) of WT adult mice before, during, and after exposure to palmitate:BSA. As shown in Figure 3, acute applications of palmitate:BSA (**Materials and Methods**) rapidly and reversibly shortened ventricular action potential durations. The mean  $\pm$  SEM action potential duration at 50% repolarization ( $\text{APD}_{50}$ ), for example, was reduced significantly ( $P < 0.05$ ) from  $5.6 \pm 1.3$  msec to  $3.2 \pm 0.5$  msec in the presence of palmitate:BSA, whereas resting membrane potentials and action potential amplitudes (Figures 3A and 3B) were not measurably affected. In addition, action potentials were measured in experiments in which  $\text{Cs}^+$  and tetraethylammonium ( $\text{TEA}^+$ ) were used in the intracellular pipette solution in place of the normal  $\text{K}^+$  to block outward  $\text{K}^+$  currents. Under these conditions, action potential waveforms were unaffected by palmitate:BSA (Figure 3A, inset), suggesting that the observed effects of palmitate:BSA on ventricular action potential durations likely reflect the modulation of repolarizing, outward  $\text{K}^+$  currents.

To examine directly the electrophysiological changes underlying action potential shortening, whole cell voltage-clamp recordings were obtained from isolated WT hearts myocytes (as described in Materials and Methods). Recording conditions were optimized to allow the measurement of either 1) repolarizing  $\text{K}^+$  currents, evoked in response to 4.5s voltage steps to test potentials between  $-60$  to  $+40$  mV from a holding potential (HP) of  $-70$  mV (with  $20 \mu\text{M}$  TTX and  $0.5 \text{ mM}$   $\text{Cd}^{2+}$  in the bath to block inward  $\text{Na}^+$  and  $\text{Ca}^{2+}$  currents, respectively); or, 2) L-type  $\text{Ca}^{2+}$  currents, evoked by 200 msec voltage steps to test potentials between  $-40$  to  $+50$  mV from a holding potential (HP) of  $-40$  mV to inactivate any residual, contaminating voltage-dependent  $\text{Na}^+$  currents (not blocked by the TTX in the bath). These experiments revealed that application of palmitate:BSA resulted in rapid increases in the amplitudes of the peak and the steady state outward  $\text{Kv}$  currents (Figure 4A). Although  $\text{Kv}$  current amplitudes were increased, neither the time- nor the voltage-dependent properties of  $I_{\text{to},f}$  or  $I_{\text{K},\text{slow}}$  were measurably affected by palmitate:BSA. In contrast, palmitate:BSA did not measurably affect the amplitudes (densities) of the inward rectifying  $\text{K}^+$  current ( $I^{\text{K1}}$ ; see Table 1) or L-type  $\text{Ca}^{2+}$  current (Figure 4B), indicating a specific effect of palmitate:BSA on  $\text{Kv}$  channels. Taken together, these results indicate that acute exposure to elevated palmitate:BSA disrupts excitation-contraction coupling in ventricular myocytes by increasing repolarizing  $\text{Kv}$  currents and shortening action potential durations.

### $\text{Kv1.5-}$ and $\text{Kv2.1-}$ Encoded $I_{\text{K},\text{slow}}$ Channels are Molecular Targets of Palmitate

The decay phases of the  $\text{Kv}$  currents in WT adult mouse left ventricular myocytes are best described by the sum of two exponentials, reflecting the co-expression of two inactivating  $\text{Kv}$  current components,  $I_{\text{to},f}$  and  $I_{\text{K},\text{slow}}$ , with markedly different inactivation kinetics [23,30].

Analysis of the voltage clamp data revealed that the relative increase in  $I_{K,slow}$  and  $I_{ss}$  amplitudes in the presence of palmitate:BSA was much larger ( $38 \pm 4\%$ , and  $35 \pm 4\%$ , respectively) than the effect on  $I_{to,f}$  amplitude ( $11 \pm 2\%$ ), suggesting that the individual Kv current components are differentially affected by palmitate:BSA. Two molecularly distinct components, encoded by the Kv1.5 and Kv2.1 pore-forming subunits, comprise mouse ventricular  $I_{K,slow}$  (now referred to as  $I_{K,slow1}$  and  $I_{K,slow2}$ ) [22,23,33,34]. Interestingly, it has previously been reported that acute exposure to elevated fatty acids affects the amplitude of heterologously expressed Kv1.5 currents [35–37], suggesting that Kv1.5-encoded  $I_{K,slow1}$  channels in mouse ventricular myocytes may be uniquely sensitive to palmitate:BSA. To explore this hypothesis directly, the effects of palmitate:BSA on Kv currents in LVA myocytes isolated from (SWAP) mice, in which the *KCNA5* (Kv1.5) locus has been replaced by *KCNA1* (Kv1.1) [22], were examined.

Previous studies have shown that  $I_{K,slow1}$ , the component of  $I_{K,slow}$  that is sensitive to  $\mu\text{M}$  concentrations of the Kv channel blocker 4-aminopyridine [38,39], is eliminated in SWAP LV myocytes [22]. The residual  $I_{K,slow}$  current,  $I_{K,slow2}$ , in SWAP myocytes is encoded by Kv2.1 and is TEA-sensitive [32]. As illustrated in Figures 5A–C, exposure of isolated SWAP LVA myocytes to palmitate:BSA also results in increased  $I_{K,slow}$  amplitudes, although the magnitude of the palmitate-induced current increase is measurably ( $\sim 50\%$ ) smaller ( $19 \pm 3\%$ ) than observed in WT ( $38 \pm 4\%$ ) myocytes (Table 1). The simplest interpretation of these results is that, although the Kv1.5-encoded  $I_{K,slow1}$  channels are an important molecular target of palmitate:BSA, the Kv2.1-encoded  $I_{K,slow2}$  channels are also affected. Consistent with this suggestion, further experiments revealed that exposure to palmitate:BSA (Figures 5A–C) also markedly increased  $I_{K,slow}$  density in LVA myocytes isolated from mice (Kv2.1<sup>-/-</sup>) harboring a targeted disruption of the *KCNB1* locus (W. Wang, N. Niwa and J.M. Nerbonne, unpublished observations). The magnitude of the increase in  $I_{K,slow}$  in Kv2.1<sup>-/-</sup> LVA myocytes ( $28 \pm 4\%$ ) is larger than in SWAP LVA myocytes (Table 1) and is approximately 75% of the magnitude of the current enhancement ( $38 \pm 4\%$ ) observed in WT LVA myocytes (Table 1). In addition, the effect of palmitate:BSA on myocyte contractility (Figure 5D) mirrors the effect on  $I_{K,slow}$ , indicating that palmitate:BSA modulates excitation-contraction coupling, in part by increasing the amplitudes of both Kv1.5- and Kv2.1-encoded components of  $I_{K,slow}$ .

### Inhibition of Voltage-Gated K<sup>+</sup> Channels Attenuates the Effects of Palmitate

To explore this relationship further, the effect of palmitate:BSA was examined in the presence of DPO-1, a previously described, reportedly selective inhibitor of Kv1.5 channels [28]. As expected, DPO-1 markedly inhibited  $I_{K,slow}$  in WT myocytes and, in addition, substantially attenuated the increase in  $I_{K,slow}$  amplitude caused by palmitate:BSA that was normally observed in the absence of DPO-1 (Figure 6A). It should also be noted that, in addition to inhibiting  $I_{K,slow}$  by 100%, DPO-1 also reduced  $I_{to,f}$  and  $I_{ss}$  amplitudes (Figure 6B) but to a lesser extent, demonstrating that although DPO-1 may be a selective blocker of Kv1.5-encoded Kv channels, it is not specific for Kv1.5 channels. In the presence of  $1 \mu\text{M}$  DPO-1 the negative inotropic effect of palmitate:BSA was significantly ( $P < 0.01$ ) attenuated, but not abolished. Because not all components of repolarizing Kv current are blocked by DPO-1, the small residual effect of palmitate:BSA on contraction is likely the consequence of effects on  $I_{to,f}$  and/or  $I_{ss}$ . Taken together, these results are consistent with the conclusion that repolarizing  $I_{K,slow}$  is a target of palmitate:BSA in ventricular myocytes and are central in mediating the observed negative inotropic effects (of palmitate:BSA).

## Discussion

### Palmitate-Dependent Attenuation of Excitation-Contraction Coupling

The objective of the present study was to examine the acute effects of palmitate on the mechanical and electrical function of ventricular cardiomyocytes. The results demonstrate that acute exposure to palmitate (complexed to BSA) transiently and reversibly inhibits myocardial contractility by reducing the  $\text{Ca}^{2+}$  transient amplitude. Interestingly, another recent study, focused on examining the responses of isolated ventricular myocytes to longer-term (20 minutes) applications of palmitate, also reported negative inotropic effects [40], consistent with the experimental observations here. The present data further demonstrate that palmitate:BSA inhibits contractility through effects on sarcolemmal membrane excitability and resulting changes in excitation-contraction coupling. Voltage-clamp recordings revealed that L-type  $\text{Ca}^{2+}$  currents are unaffected by palmitate:BSA, whereas voltage-dependent outward  $\text{K}^+$  currents are increased significantly on acute exposures to palmitate:BSA, resulting in action potential shortening. The augmentation of repolarizing  $\text{K}^+$  currents and the attenuation of action potential durations lead to reductions in voltage-dependent  $\text{Ca}^{2+}$  influx (and  $\text{Ca}^{2+}$ -dependent release of  $\text{Ca}^{2+}$  from intracellular stores) and to decreased myocyte contractility.

It is well established that nearly all of the non-esterified fatty acid in serum is bound to lipid carrying proteins, including *albumin* [41]. This situation was mimicked in the experiments here by examining the effects of palmitate complexed to BSA at a constant 1:2 molar ratio. At a fixed ratio, regardless of the absolute amounts of palmitate and BSA, the same final unbound palmitate concentration of 42 nM is predicted [25]. Despite this, a marked “concentration-dependent” effect of palmitate:BSA on contractility was observed (Figure 1D). That is, when both palmitate and BSA were increased, maintaining a fixed molar ratio (and the same calculated free palmitate concentration), contractility was inhibited to a greater degree. These observations could be interpreted as suggesting that BSA alone inhibits contraction. Control experiments revealed, however, that in the absence of palmitate, BSA has no measurable effects on either contractility or membrane excitability (Figure 1, Table 1). It can be inferred, then, that the free palmitate is not solely determined by the BSA:palmitate ratio and/or that BSA affects the manner in which palmitate is imported into the cell. Indeed, previous studies demonstrated that the rate of palmitate uptake increases as a function of the total palmitate concentration at a fixed palmitate:BSA molar ratio, observations consistent with the results presented here [41]. In the same study, it was also demonstrated that the rate of palmitate uptake is dependent on rapid intracellular metabolism such that most of the imported palmitate is rapidly metabolized [41]. These findings further suggest that the bioactive lipid in the studies described here might not be palmitate per se, but rather a metabolic intermediate. Further studies, using alternative experimental approaches, would be required to explore this hypothesis directly. Regardless, the data presented here demonstrate that acute exposure to palmitate, whether acting directly or indirectly (by functioning as a metabolic precursor), increases  $\text{Kv}$  current density and inhibits myocyte contraction.

### Metabolic sensitivity of $\text{Kv}$ channels

The results of the present studies support the conclusion that the negative inotropic effects of palmitate:BSA result from increased  $\text{Kv}$  currents. Accordingly, when  $\text{Kv}$  currents are reduced, using either pharmacological blockers (such as DPO-1) or homologous recombination (SWAP or  $\text{Kv}2.1^{-/-}$  mice) to reduce the densities of functional  $\text{Kv}$  channels selectively, the effects of palmitate on  $\text{Kv}$  currents and on contractility are markedly attenuated in parallel. In previous studies, focused on examining the effects of palmitate on myocyte contractility and intracellular  $\text{Ca}^{2+}$  signals, Fauconnier and colleagues reported that the negative inotropic effects of palmitate were reversed by N-acetyl cysteine, suggesting a possible role for reactive oxygen species [40]. These observations further suggest that the uptake and metabolism of palmitate



are necessary for the observed functional effects and, in addition, that the effects of palmitate on Kv channels reflect an intracellular site of action. Interestingly, in the experiments here, palmitate:BSA application increased Kv current densities without measurably affecting the time- and/or voltage-dependent properties of the currents. This finding is reminiscent of the reported increase in the amplitudes of the 4-aminopyridine-sensitive Kv currents, without measurable effects on the time- and/or voltage-dependent properties of the currents, in canine coronary smooth muscle in response to H<sub>2</sub>O<sub>2</sub> [42]. Similarly, an H<sub>2</sub>O<sub>2</sub>-dependent hyperpolarization of Aplysia sensory neurons has been shown to be blocked by TEA, indicating Kv channel involvement [43]. In addition, H<sub>2</sub>O<sub>2</sub> also reportedly increased recombinant Kv1.5 channels expressed in a mammalian cell line, although in these experiments, the voltage-dependent properties of the currents were also affected [44]. Other previous studies have demonstrated Kv current inhibition in response to reactive oxygen species [45]. Interestingly, the Kv channel accessory subunit, Kvβ1, has recently been shown to be a catalytically active member of the aldo-keto reductase family of proteins [46,47]. Taken together, these observations suggest the interesting possibility that Kvβ1 might function to modulate Kv channel activity in response to redox state and/or to changes in NADP<sup>+</sup>/NADPH ratios, i.e., Kvβ1 subunits may function to confer metabolic sensitivity on Kv channels.

### Elevated Fatty Acids and Augmentation of Kv Currents

There have been surprisingly few studies that have examined the physiological effects of excess palmitate under conditions in which metabolism is not also inhibited by hypoxia or ischemia. The action potential shortening observed in the present study mirrors results obtained by others in whole tissue preparations. Palmitate (0.84 or 1.3 mM, complexed to 2% BSA), for example, has been shown to cause action potential shortening in papillary muscle [48]. Similarly, Willebrands and colleagues reported that perfusion of the isolated rat heart with palmitate (1–3 mM, complexed with 0.66 mM BSA) induced arrhythmias and reduced contractility in agreement with the present data [49]. In addition, previous electrophysiological studies on metabolically compromised tissues (e.g. hypoxia, low-flow ischemia) in a number of species have shown, similar to the present study, that palmitate shortens action potential durations and reduces contractility.

To our knowledge, there have been no previously described studies that have specifically examined the effects of palmitate on the functional expression of myocardial Kv currents. The increases in Kv current densities observed here could reflect increased targeting of assembled channels to the sarcolemmal membrane or, perhaps, to lipid rafts. Recent studies indicate that palmitoylation of Kv1.5 may be important for channel trafficking and localization [50,51]. The present data neither support nor refute the notion that such a mechanism occurs in cardiac myocytes; however, the acute and reversible nature of the observed increases in voltage-dependent K<sup>+</sup> currents is inconsistent with the observation that palmitoylation occurs on newly synthesized protein [50].

In contrast to the negative inotropic effects of the saturated fatty acid palmitate presented in this study, polyunsaturated fatty acids have been reported to have cardioprotective and antiarrhythmic effects. In addition, both polyunsaturated fish oils (ω-3 fatty acids) and linoleic acid (polyunsaturated ω-6 fatty acid) have been shown to block Kv1.5 channels [35,37], effects that would also lead to action potential prolongation. The effects of linoleic acid, however, may be complex, as other studies suggest that linoleic acid both inhibits and activates Kv1.5- (as well as Kv2.1-) encoded myocardial Kv channels [36].

### Lipid Homeostasis and Cardiac Diseases

Derangement of both cardiac and systemic lipid homeostasis is a key feature of diabetes mellitus [9,52]. The hypothesis driving the studies described here was that elevated systemic

free fatty acid concentrations in individuals with diabetes impair cardiac contractile function. The experiments revealed a negative inotropic effect of acute fatty acid application that is consistent with this notion. In recent previous studies, we have shown that increased cardiac-specific storage and usage of lipids, driven by the overexpression of FATP1 in the heart specifically impairs diastolic function [10,11], recapitulating an early onset feature of the disease. In comparison, the negative inotropic effect of palmitate observed in the present study is consistent with a potentially causative (and direct) role for systemic lipid derangements in systolic dysfunction observed in diabetic cardiomyopathy. By augmenting Kv currents, palmitate: BSA shortens action potential durations, inhibits excitation-contraction coupling and impairs systolic myocyte function.

It is also important to emphasize that the focus of this study was on exploring the short term effects on excitation-contraction coupling of exposure to elevated extracellular palmitate and the underlying cellular mechanisms involved in mediating these effects. These experiments revealed that the observed alterations in contractility reflect palmitate-induced augmentation of repolarizing Kv currents. The applicability of the results obtained in the experiments here to those produced by chronic elevations in free fatty acid concentrations remains to be determined. Long-term exposures to elevated free fatty acids *in vivo* might well lead to compensatory responses, such as remodeling of  $I_{Ca}$  [24] or of contractile filaments [11], thereby ameliorating some of the observed (acute) effects on Kv currents and/or on contractility directly. The present study was limited to exploring the acute effects of palmitate on mouse ventricular myocytes, primarily because genetic manipulations can be made readily in the mouse, thereby facilitating mechanistic studies. Importantly, the experiments here revealed that acute exposure to elevated palmitate results in the remodeling of repolarizing Kv channels. In larger mammals, a repertoire of repolarizing Kv currents that are likely to be similarly affected by palmitate is also expressed. This hypothesis warrants critical testing. Finally, the action potential shortening observed in these experiments might be expected to shorten  $QT_c$  intervals. Conversely,  $QT_c$  prolongation (not shortening) is often observed in patients with Type 1, as well as Type 2, Diabetes [53,54]. This apparent discordance could again reflect compensatory responses *in vivo* or perhaps alterations in the functioning of the autonomic nervous system [55], neither of which was a factor in this study.

It should also be pointed out that derangements in lipid metabolism are not limited to diabetes, and acute elevations of circulating fatty acids can be triggered during myocardial ischemia [56]. The experimental paradigm that we have used may actually be more applicable to this situation, where there is a surge of fatty acid release into the blood. Interestingly, there is substantial evidence that increased circulating free fatty acid levels are correlated with arrhythmia incidence in the ischemic heart [57,58]. The sequelae of myocardial ischemia are obviously complex, involving metabolism, neuro-hormonal signaling, and hemodynamic changes. Even given these complexities, the present data suggest that palmitate-induced action potential shortening could facilitate the development of re-entrant tachycardias during and immediately following acute myocardial ischemia.

## Conclusions

There is mounting evidence that cardiac metabolism and disease are intimately related. In this regard, altered energy metabolism is a prominent feature of, and in some instances may cause, heart failure [1,2]. The results of the studies detailed here demonstrate the importance of lipid metabolism in cardiac electrical and mechanical functioning. Acute exposure to elevated palmitate complexed to BSA disrupts excitation contraction coupling and impairs myocardial contractility. As such, elevations in circulating saturated fatty acids, such as those that may occur in diabetes mellitus or myocardial ischemia, can potentially have an immediate, as well as a long-term, impact on both electrical and contractile function of the heart.

## Acknowledgments

The authors wish to thank Ms. Amy Coleman for expert technical assistance in the isolation of adult mouse ventricular myocytes and Rick Wilson for maintaining and screening the mouse colony. In addition, the financial support provided by the Washington University-Pfizer Biomedical Research Program and the Heartland Affiliate of the American Heart Association (Postdoctoral Fellowship to Wei Wang) is gratefully acknowledged.

## References

1. Ashrafian H, Frenneaux MP, Opie LH. Metabolic mechanisms in heart failure. *Circulation* 2007;116:434–448. [PubMed: 17646594]
2. Boudina S, Abel ED. Diabetic cardiomyopathy revisited. *Circulation* 2007;115:3213–3223. [PubMed: 17592090]
3. Kannel WB, Hjortland M, Castelli WP. Role of diabetes in congestive heart failure: the Framingham study. *Am J Cardiol* 1974;34:29–34. [PubMed: 4835750]
4. Regan TJ, Lyons MM, Ahmed SS, Levinson GE, Oldewurtel HA, Ahmad MR, Haider B. Evidence for cardiomyopathy in familial diabetes mellitus. *J Clin Invest* 1977;60:884–899. [PubMed: 893679]
5. Stanley WC, Lopaschuk GD, McCormack JG. Regulation of energy substrate metabolism in the diabetic heart. *Cardiovas Res* 1997;34:25–33.
6. Belke DD, Larsen TS, Lopaschuk GD, Severson DL. Glucose and fatty acid metabolism in the isolated working mouse heart. *Am J Physiol* 1999;277:R1210–R1217. [PubMed: 10516264]
7. Frazee E, Donner CC, Swislocki AL, Chiou YA, Chen YD, Reaven GM. Ambient plasma free fatty acid concentrations in noninsulin-dependent diabetes mellitus: evidence for insulin resistance. *J Clin Endocrinol Metab* 1985;61:807–811. [PubMed: 3900120]
8. Lopaschuk GD. Metabolic abnormalities in the diabetic heart. *Heart Failure Reviews* 2002;7:149–159. [PubMed: 11988639]
9. Belke DD, Larsen TS, Gibbs EM, Severson DL. Altered metabolism causes cardiac dysfunction in perfused hearts from diabetic (*db/db*) mice. *Am J Physiol* 2000;279:E1104–E1113.
10. Chiu HC, Kovacs A, Blanton RM, Han X, Courtois M, Weinheimer CJ, Yamada KA, Brunet S, Xu H, Nerbonne JM, Welch MJ, Fettig NM, Sharp TL, Sambandan N, Olson KM, Ory D, Schaffer JE. Transgenic expression of fatty acid transport protein 1 in the heart causes lipotoxic cardiomyopathy. *Circ Res* 2005;96:225–233. [PubMed: 15618539]
11. Flagg TP, Cazorla O, Remedi MS, Haim TE, Tones MA, Bahinski A, Numann RE, Kovacs A, Schaffer JE, Nichols CG, Nerbonne JM.  $Ca^{2+}$ -independent alterations in diastolic sarcomere length and relaxation kinetics in a mouse model of lipotoxic diabetic cardiomyopathy. *Circ Res* 2009;104:95–103. [PubMed: 19023131]
12. Liu JE, Palmieri V, Roman MJ, Bella JN, Fabsitz R, Howard BV, Welty TK, Lee ET, Devereux RB. The impact of diabetes on left ventricular filling pattern in normotensive and hypertensive adults: the strong heart study. *J Am Coll Cardiol* 2001;37:1943–1949. [PubMed: 11401136]
13. Diamant M, Lamb HJ, Groeneveld Y, Endert EL, Smit JWA, Bax JJ, Romijn JA, deRoos A, Radder JK. Diastolic dysfunction is associated with altered myocardial metabolism in asymptomatic normotensive patients with well-controlled type 2 diabetes mellitus. *J Am Coll Cardiol* 2003;42:328–335. [PubMed: 12875772]
14. Bella JN, Devereux RB, Roman MJ, Palmieri V, Liu JE, Paranicas M, Welty TK, Lee ET, Fabsitz RR, Howard BV. Separate and joint effects of systemic hypertension and diabetes mellitus on left ventricular structure and function in American Indians (the Strong Heart Study). *Am J Cardiol* 2001;87:1260–1265. [PubMed: 11377351]
15. Devereux RB, Roman MJ, Paranicas M, O'Grady MJ, Lee ET, Welty TK, Fabsitz RR, Robbins D, Rhoades ER, Howard BV. Impact of Diabetes on Cardiac Structure and Function: The Strong Heart Study. *Circulation* 2000;101:2271–2276. [PubMed: 10811594]
16. Aneja A, Tang WHW, Bansilal S, Garcia MJ, Farkouh ME. Diabetic cardiomyopathy: insights into pathogenesis, diagnostic challenges, and therapeutic options. *Am J Med* 2008;121:748–757. [PubMed: 18724960]
17. Paradise NF, Pilati CF, Payne WR, Finkelstein JA. Left ventricular function of the isolated, genetically obese rat's heart. *Am J Physiol* 1985;248:H438–H444. [PubMed: 3985169]

18. Joffe II, Travers KE, Perreault-Micale CL, Hampton T, Katz SE, Morgan JP, Douglas PS. Abnormal cardiac function in the streptozotocin-induced, non-insulin-dependent diabetic rat: Noninvasive assessment with Doppler echocardiography and contribution of the nitric oxide pathway. *J Am Coll Cardiol* 1999;34:2111–2119. [PubMed: 10588232]
19. Young ME, Guthrie PH, Razeghi P, Leighton B, Abbasi S, Patil S, Youker KA, Taegtmeier H. Impaired long-chain fatty acid oxidation and contractile dysfunction in the obese Zucker rat heart. *Diabetes* 2002;51:2587–2595. [PubMed: 12145175]
20. An D, Rodrigues B. Role of changes in cardiac metabolism in development of diabetic cardiomyopathy. *Am J Physiol* 2006;291:H1489–H1506.
21. Zhou YT, Grayburn P, Karim A, Shimabukuro M, Higa M, Baetens D, Orci L, Unger RH. Lipotoxic heart disease in obese rats: implications for human obesity. *Proc Natl Acad Sci U S A* 2000;97:1784–1789. [PubMed: 10677535]
22. London B, Guo W, Pan X, Lee JS, Shusterman V, Rocco CJ, Logothetis DA, Nerbonne JM, Hill JA. Targeted replacement of Kv1.5 in the mouse leads to loss of the 4-aminopyridine-sensitive component of I(K,s) and resistance to drug-induced QT prolongation. *Circ Res* 2001;88:940–946. [PubMed: 11349004]
23. Xu H, Guo W, Nerbonne JM. Four kinetically distinct depolarization-activated K<sup>+</sup> currents in adult mouse ventricular myocytes. *J Gen Physiol* 1999;113:661–678. [PubMed: 10228181]
24. Flagg TP, Charpentier F, Manning-Fox J, Remedi MS, Enkvetchakul D, Lopatin A, Koster J, Nichols CG. Remodeling of excitation-contraction coupling in transgenic mice expressing ATP-insensitive sarcolemmal K-ATP channels. *Am J Physiol* 2004;286:H1361–H1369.
25. Richieri GV, Anel A, Kleinfeld AM. Interactions of long-chain fatty acids and albumin: determination of free fatty acid levels using the fluorescent probe ADIFAB. *Biochemistry* 1993;32:7574–7580. [PubMed: 8338853]
26. Listenberger LL, Ory DS, Schaffer JE. Palmitate-induced apoptosis can occur through a ceramide-independent pathway. *J Biol Chem* 2001;276:14890–14895. [PubMed: 11278654]
27. Kleinfeld AM, Prothro D, Brown DL, Davis RC, Richieri GV, DeMaria A. Increases in serum unbound free fatty acid levels following coronary angioplasty. *Am J Cardiol* 1996;78:1350–1354. [PubMed: 8970405]
28. Lagrutta A, Wang J, Fermini B, Salata JJ. Novel, Potent inhibitors of human Kv1.5 K<sup>+</sup> channels and ultrarapidly activating delayed rectifier potassium current. *J Pharmacol Exper Ther* 2006;317:1054–1063. [PubMed: 16522807]
29. Di VF, Steinberg TH, Silverstein SC. Inhibition of Fura-2 sequestration and secretion with organic anion transport blockers. *Cell Calcium* 1990;11:57–62. [PubMed: 2191781]
30. Brunet S, Aimond F, Li H, Guo W, Eldstrom J, Fedida D, Yamada KA, Nerbonne JM. Heterogeneous expression of repolarizing, voltage-gated K<sup>+</sup> currents in adult mouse ventricles. *J Physiol* 2004;559:103–120. [PubMed: 15194740]
31. Fauconnier J, Andersson DC, Zhang SJ, Lanner JT, Wibom R, Katz A, Bruton JD, Westerblad H. Effects of palmitate on Ca<sup>2+</sup> handling in adult control and ob/ob cardiomyocytes: impact of mitochondrial reactive oxygen species. *Diabetes* 2007;56:1136–1142. [PubMed: 17229941]
32. Bers DM. Cardiac excitation-contraction coupling. *Nature* 2002;415:198–205. [PubMed: 11805843]
33. Li H, Guo W, Yamada KA, Nerbonne JM. Selective elimination of I<sub>K,s1</sub> in mouse ventricular myocytes expressing a dominant negative Kv1.5a subunit. *Am J Physiol* 2004;286:H319–H328.
34. Kodirov SA, Brunner M, Nerbonne JM, Buckett P, Mitchell GF, Koren G. Attenuation of I<sub>K,s1</sub> and I<sub>K,s2</sub> in Kv1/Kv2DN mice prolongs APD and QT intervals but does not suppress spontaneous or inducible arrhythmias. *Am J Physiol* 2004;286:H368–H374.
35. Honore E, Barhanin J, Attali B, Lesage F, Lazdunski M. External blockade of the major cardiac delayed-rectifier K<sup>+</sup> channel (Kv1.5) by polyunsaturated fatty acids. *Proc Natl Acad Sci U S A* 1994;91:1937–1941. [PubMed: 8127910]
36. McKay MC, Worley JF III. Linoleic acid both enhances activation and blocks Kv1.5 and Kv2.1 channels by two separate mechanisms. *Am J Physiol* 2001;281:C1277–C1284.
37. Guizy M, David M, Arias C, Zhang L, Cofbn M, Ruiz-Gutierrez V, Ros E, Lillo MP, Martens JR, Valenzuela C. Modulation of the atrial specific Kv1.5 channel by the n-3 polyunsaturated fatty acid, [alpha]-linolenic acid. *J Mol Cell Cardiol* 2008;44:323–335. [PubMed: 18155022]

38. Fiset C, Clark RB, Larsen TS, Giles WR. A rapidly activating sustained K<sup>+</sup> current modulates repolarization and excitation-contraction coupling in adult mouse ventricle. *J Physiol* 1997;504:557–563. [PubMed: 9401964]
39. London B, Wang DW, Hill JA, Bennett PB. The transient outward current in mice lacking the potassium channel gene Kv1.4. *J Physiol* 1998;509(Pt 1):171–182. [PubMed: 9547391]
40. Fauconnier J, Andersson DC, Zhang S-J, Lanner JT, Wibom R, Katz A, Bruton JD, Westerblad H. Effects of pslmitste on Ca<sup>2+</sup> handling in adult control and *ob/ob* cardiomyocytes. *Diabetes* 2007;56:1136–1142. [PubMed: 17229941]
41. Luiken JJ, van Nieuwenhoven FA, America G, van der Vusse GJ, Glatz JF. Uptake and metabolism of palmitate by isolated cardiac myocytes from adult rats: involvement of sarcolemmal proteins. *J Lipid Res* 1997;38:745–758. [PubMed: 9144089]
42. Rogers PA, Chilian WM, Bratz IN, Bryan RM Jr, Dick GM. H<sub>2</sub>O<sub>2</sub> activates redox- and 4-aminopyridine-sensitive Kv channels in coronary vascular smooth muscle. *Am J Physiol* 2007;292:H1404–H1411.
43. Chang DJ, Lim CS, Lee SH, Kaang BK. Hydrogen peroxide modulates K<sup>+</sup> ion currents in cultured Aplysia sensory neurons. *Brain Res* 2003;970:159–168. [PubMed: 12706257]
44. Caouette D, Dongmo C, Berube J, Fournier D, Daleau P. Hydrogen peroxide modulates the Kv1.5 channel expressed in a mammalian cell line. *Naunyn Schmiedebergs Arch Pharmacol* 2003;368:479–486. [PubMed: 14614593]
45. Duprat F, Guillemare E, Romey G, Fink M, Lesage F, Lazdunski M, et al. Susceptibility of cloned K<sup>+</sup> channels to reactive oxygen species. *Proc Natl Acad Sci U S A* 1995;92:11796–11800. [PubMed: 8524851]
46. Tipparaju SM, Barski OA, Srivastava S, Bhatnagar A. Catalytic mechanism and substrate specificity of the β-subunit of the voltage-gated potassium channel. *Biochemistry* 2008;47:8840–8854. [PubMed: 18672894]
47. Weng J, Cao Y, Moss N, Zhou M. Modulation of voltage-dependent *Shaker* family potassium channels by an aldo-keto reductase. *J Biol Chem* 2006;281:15194–15200. [PubMed: 16569641]
48. Luderitz B, Naumann dC, Steinbeck G. Effects of free fatty acids on electrophysiological properties of ventricular myocardium. *Klin Wochenschr* 1976;54:309–313. [PubMed: 1263406]
49. Willebrands AF, Tasseront JA, ter Welle HF, van Dam RT. Effects of oleic acid and oxygen restriction followed by re-oxygenation on rhythm and contractile activity of the isolated rat heart; protective action of glucose. *J Mol Cell Cardiol* 1976;8:375–388. [PubMed: 940166]
50. Jindal HK, Folco EJ, Liu GX, Koren G. Posttranslational modification of voltage-dependent potassium channel Kv1.5: COOH-terminal palmitoylation modulates its biological properties. *Am J Physiol* 2008;294:H2012–H2021.
51. Zhang L, Foster K, Li Q, Martens JR. S-acylation regulates Kv1.5 channel surface expression. *Am J Physiol* 2007;293:C152–C161.
52. Carley AN, Severson DL. Fatty acid metabolism is enhanced in type 2 diabetic hearts. *Biochim Biophys Acta: Molecular and Cell Biology of Lipids* 2005;1734:112–126.
53. Giunti S, Bruno G, Lillaz E, Gruden G, Lolli V, Chaturvedi N, et al. Incidence and risk factors of prolonged QTc interval in type 1 diabetes: the EURODIAB Prospective Complications Study. *Diabetes Care* 2007;30:2057–2063. [PubMed: 17485572]
54. Veglio M, Bruno G, Borra M, Macchia G, Bargero G, D'Errico N, et al. Prevalence of increased QT interval duration and dispersion in type 2 diabetic patients and its relationship with coronary heart disease: a population-based cohort. *J Intern Med* 2002;251:317–324. [PubMed: 11952882]
55. Pappachan JM, Sebastian J, Bino BC, Jayaprakash K, Vijayakumar K, Sujathan P, et al. Cardiac autonomic neuropathy in diabetes mellitus: prevalence, risk factors and utility of corrected QT interval in the ECG for its diagnosis. *Postgrad Med J* 2008;84:205–210. [PubMed: 18424578]
56. Oliver MF, Kurien VA, Greenwood TW. Relation between serum-free-fatty acids and arrhythmias and death after acute myocardial infarction. *Lancet* 1968;1:710–714. [PubMed: 4170959]
57. Oliver MF, Opie LH. Effects of glucose and fatty acids on myocardial ischaemia and arrhythmias. *Lancet* 1994;343:155–158. [PubMed: 7904009]
58. Davies NJ, Lovlin RE, Lopaschuk GD. Effect of exogenous fatty acids on reperfusion arrhythmias in isolated working perfused hearts. *Am J Physiol* 1992;262:H1796–H1801. [PubMed: 1621838]

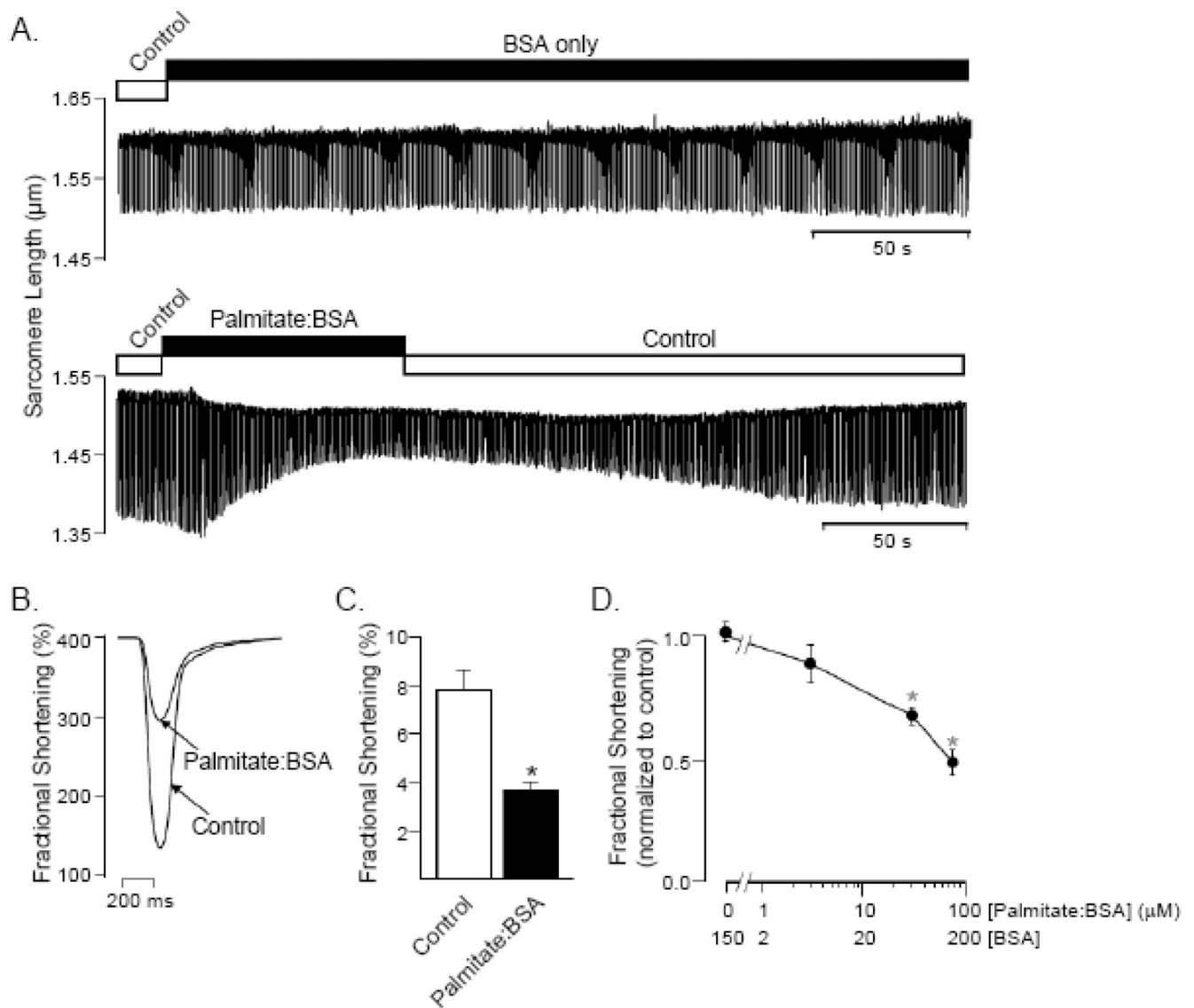


**Figure 1.**

Palmitate alters sarcomere mechanics in a concentration-dependent manner. (A) Representative recordings of sarcomere shortening in adult (wild type mouse) ventricular myocytes recorded stimulated at 1Hz and during superfusion with control Tyrode solution or Tyrode solution containing BSA (top panel) or palmitate: BSA (lower panel). (B) Single contraction record obtained from the experiment in (A) during exposure to control Tyrode and to palmitate:BSA, immediately prior to washout. (C) Although BSA has no measurable effects on contractility, exposure to palmitate:BSA significantly ( $P < 0.05$ ; paired t-test), reduced mean  $\pm$  SEM ( $n = 28$ ) fractional shortening in a concentration-dependent manner (D). \*Values are significantly ( $P < 0.05$ ) different from controls.

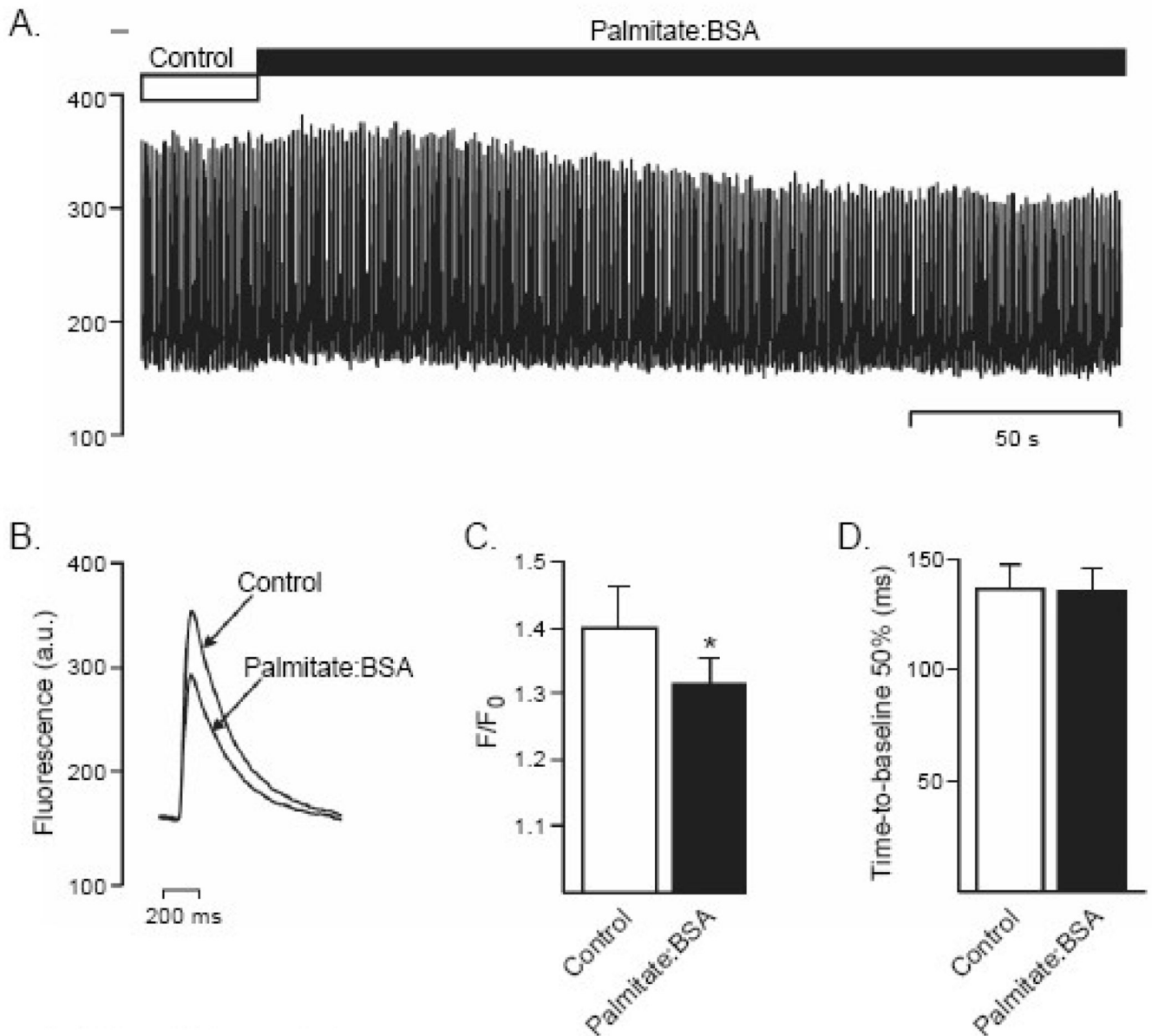


**Figure 2.**

Palmitate reduces intracellular  $\text{Ca}^{2+}$  transients. (A) Representative calcium transients recorded in WT adult mouse ventricular myocytes stimulated at 20V and 1Hz during bath perfusion of control Tyrode solution or Tyrode solution containing palmitate:BSA. (B) Average  $\text{Ca}^{2+}$  transient data obtained from the experiment in (A) during control Tyrode and palmitate:BSA applications. (C) The mean  $\pm$  SEM ( $n = 12$ ) peak height of the calcium transient ( $F/F_0$ ) was reduced significantly ( $* P < 0.05$ , paired t-test), by palmitate:BSA, whereas the time course of  $\text{Ca}^{2+}$  removal from the cytosol (D) was unaffected.

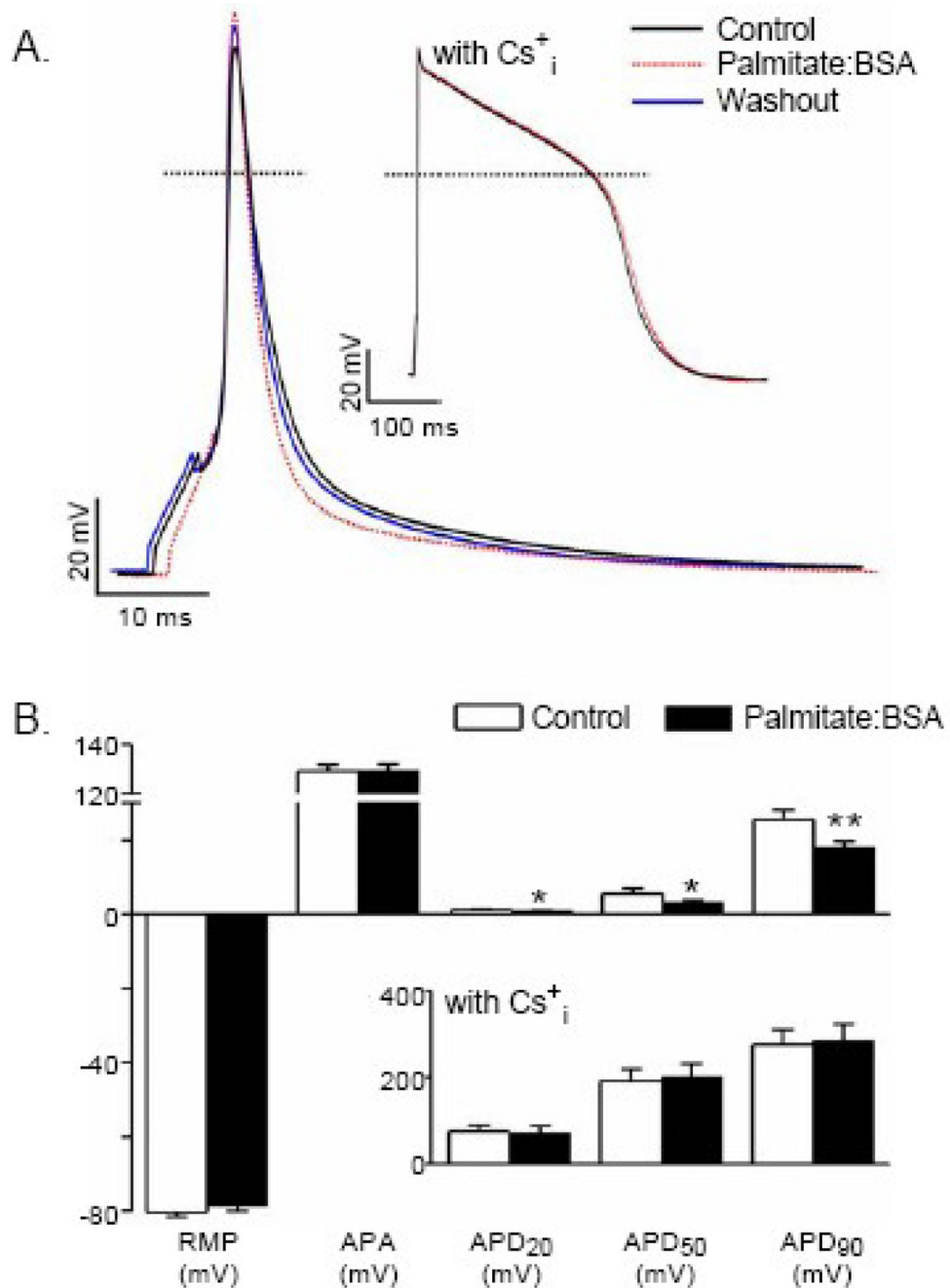


**Figure 3.** Palmitate shortens action potential durations in WT adult mouse left ventricular apex (LVA) myocytes. (A) Representative whole-cell action potentials, evoked by brief (4 ms) suprathreshold current injections, presented at 15s intervals, recorded before (black), during (dotted red) and following (blue) washout of palmitate:BSA (30  $\mu\text{M}$ :60  $\mu\text{M}$ ) solution. Dotted horizontal lines indicate the 0 voltage levels. The action potential shown in the inset (labeled with  $\text{Cs}^+_i$ ) was recorded from a WT LVA myocyte with  $\text{Cs}^+$  and TEA in the pipette solution in place of the normal  $\text{K}^+$  solution (to block outward  $\text{K}^+$  currents). (B) Mean  $\pm$  SEM resting membrane potentials and action potential amplitudes in recordings obtained with normal ( $n=18$ ) intracellular  $\text{K}^+$  and with  $\text{K}^+$ -free ( $n=14$ ) pipette solutions are not measurably affected



by application of palmitate:BSA. Mean  $\pm$  SEM action potential durations at 20% (APD<sub>20</sub>), at 50% (APD<sub>50</sub>) and at 90% (APD<sub>90</sub>) repolarization recorded with normal (n=18) K<sup>+</sup>-containing pipette solution, however, are significantly (\**P*<0.05, \*\**P*<0.01 versus control; paired t test) reduced following exposure to palmitate:BSA. With Cs<sup>+</sup> in the recording pipettes (inset) to block outward K<sup>+</sup> currents, in contrast, mean  $\pm$  SEM (n=14) APD<sub>20</sub>, APD<sub>50</sub> and APD<sub>90</sub> values in LVA myocytes are not measurably affected by palmitate:BSA.

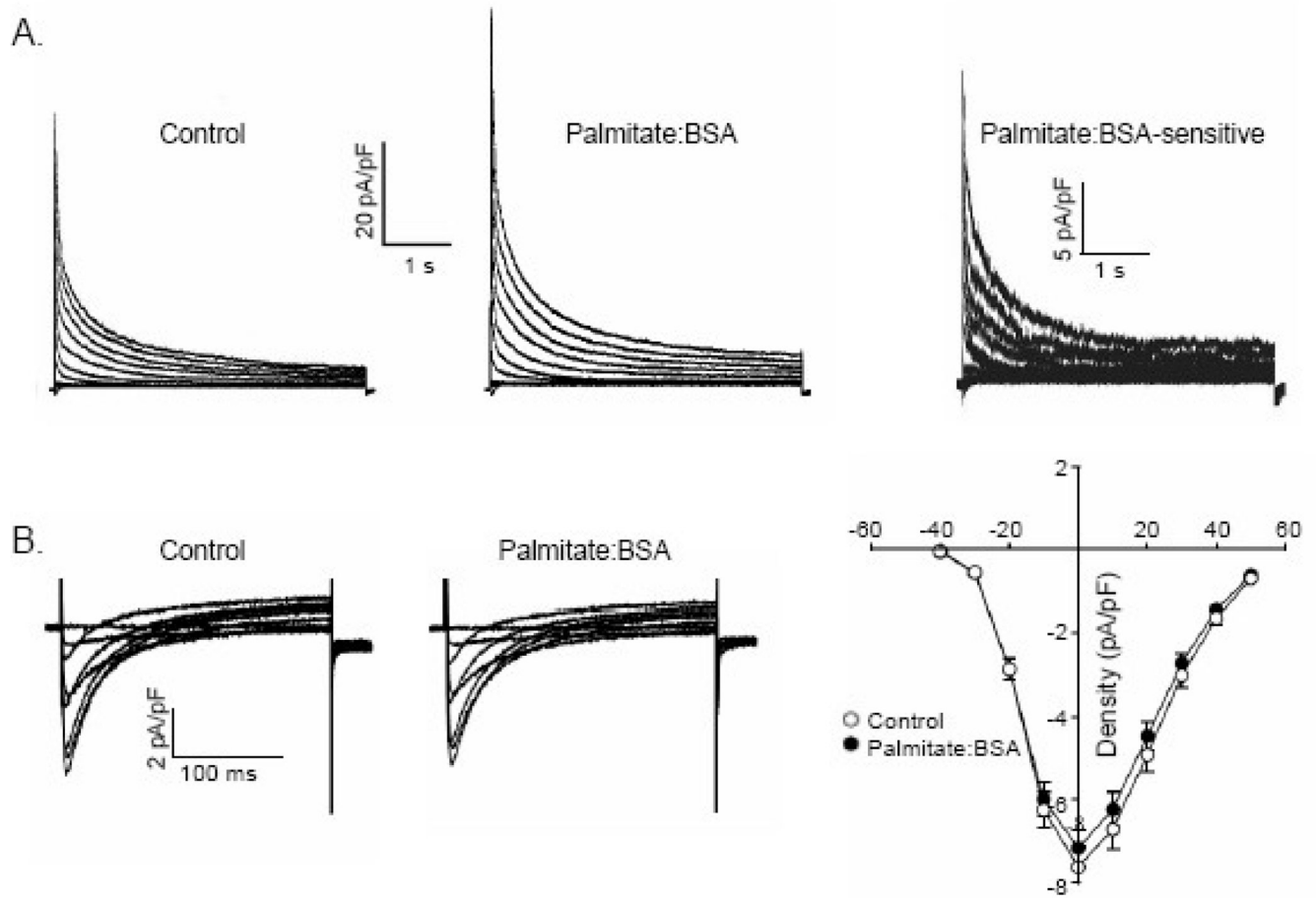


**Figure 4.**

Palmitate augments repolarizing, voltage-gated  $K^+$  ( $K_v$ ) currents, but does not affect voltage-gated  $Ca^{2+}$  currents, in WT LVA myocytes. (A) Representative whole-cell voltage-gated  $K^+$  ( $K_v$ ) currents, recorded in response to a series of 4.5s voltage steps (to test potentials ranging from  $-60$  to  $+40$  mV) from a holding potential of  $-70$  mV are displayed; voltage steps were presented in 10 mV increments at 15s intervals. Outward  $K_v$  currents were increased on superfusion of bath solution containing palmitate:BSA ( $30 \mu\text{M}:60 \mu\text{M}$ ); the palmitate-sensitive currents were obtained by subtraction of the currents recorded in the presence of palmitate from those recorded before application of palmitate (in the same cell). (B) Representative whole-cell voltage-gated  $Ca^{2+}$  currents, recorded in response to 250 ms voltage steps from a holding potential of  $-70$  mV to test potentials between  $-40$  and  $+50$  mV are displayed; voltage steps were presented in 10 mV increments at 15s intervals. Inward  $Ca^{2+}$  currents were unaffected by superfusion of bath solutions containing palmitate:BSA ( $30 \mu\text{M}:60 \mu\text{M}$ ); Mean  $\pm$  SEM  $Ca^{2+}$  current amplitudes ( $n=14$ ) in control and palmitate:BSA, plotted as a function of test potential, are indistinguishable.

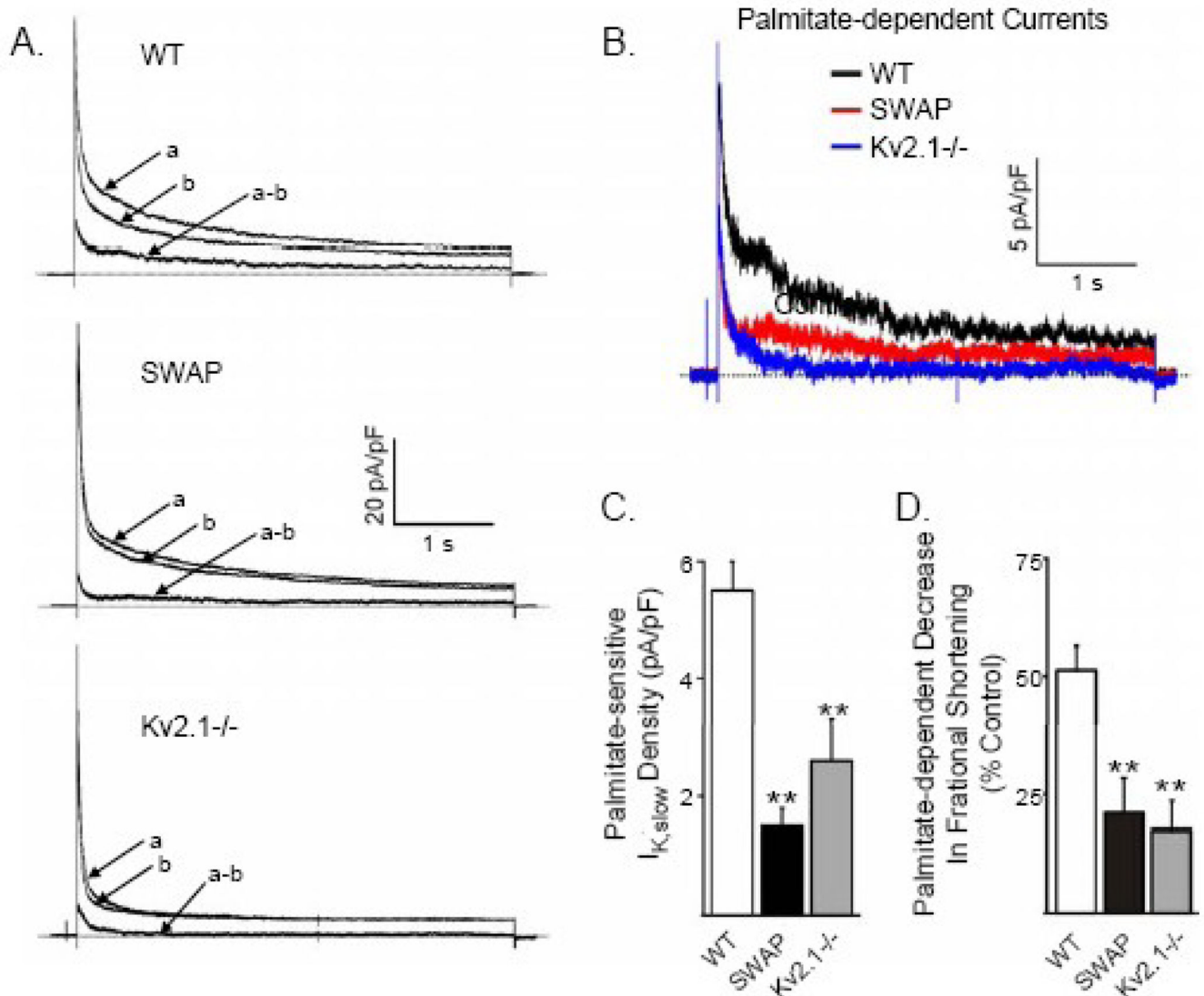


**Figure 5.**

Selective loss of  $I_{K,slow}$  in SWAP and Kv2.1<sup>-/-</sup> ventricular myocytes reduces palmitate-sensitive  $K^+$  currents. (A) Outward  $K^+$  currents, evoked in response to 4.5 s voltage steps from a holding potential of  $-70$  mV to  $+40$  mV at 15 s intervals, were recorded from WT, SWAP and Kv2.1<sup>-/-</sup> LVA myocytes under control conditions (a) and following superfusion of palmitate:BSA (30  $\mu$ M:60  $\mu$ M)(b). The amplitudes of the outward  $K^+$  currents in LVA myocytes isolated from WT, SWAP and Kv2.1<sup>-/-</sup> mice were increased on application of palmitate:BSA. The palmitate-sensitive currents (a-b) were obtained by off-line digital subtraction of the currents recorded in palmitate:BSA (b) from the control (a) records in the same cell. (B) Comparison of the waveforms of the palmitate-sensitive  $K^+$  currents in WT (black), SWAP (red) and Kv2.1<sup>-/-</sup> (blue) LVA myocytes. The mean  $\pm$  SEM densities of the palmitate-sensitive outward  $K^+$  currents (C) and the palmitate dependent decrease in fractional shortening (D) are significantly (\*\* $P < 0.01$ ) lower in SWAP and in Kv2.1<sup>-/-</sup>, than in WT, LVA myocytes.

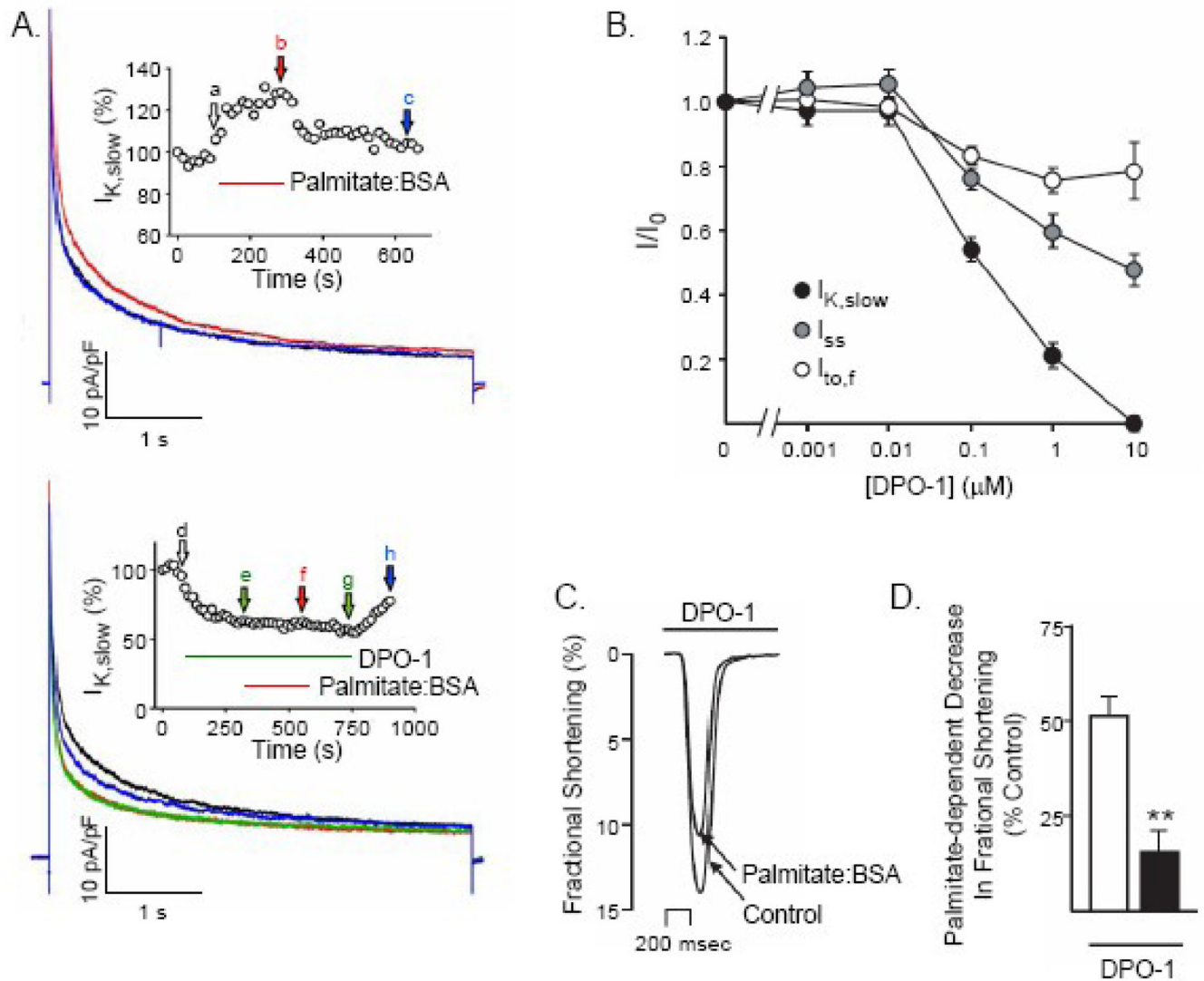


**Figure 6.**

Pharmacological inhibition of  $I_{K,slow}$  by DPO-1 occludes the effects of palmitate on ventricular Kv currents and fractional shortening. (A) Representative Kv current recordings from a WT myocyte in response to depolarizing voltage steps to +40 mV from a holding potential of -70 mV, presented at 15 s intervals; currents recorded during superfusion of control solution (black), palmitate:BSA (30  $\mu$ M:60  $\mu$ M) (red) and following washout (blue) are displayed.  $I_{K,slow}$  was reversibly increased by palmitate. Inset:  $I_{K,slow}$  amplitude (normalized to control) is plotted as a function of time during the application and washout of palmitate:BSA. (B) Representative Kv currents recorded from a WT myocyte in response to depolarizing voltage steps +40 mV as described in (A) in control bath solution (black), following superfusion of 100 nM DPO-1 (green) or 100 nM DPO-1 plus palmitate:BSA (30  $\mu$ M:60  $\mu$ M) (red) and after washout (blue), are displayed. The addition of palmitate:BSA in the presence of DPO-1 does not measurably affect the amplitudes or the waveforms of the Kv currents. Inset:  $I_{K,slow}$  amplitude (normalized to control) is plotted as a function of time during the application and washout of DPO-1 and DPO-1 plus palmitate:BSA. (C) Analyses of the Kv currents revealed that, in addition to inhibiting of  $I_{K,slow}$ , DPO-1 also attenuates the amplitudes of the transient ( $I_{to,f}$ ) and steady state ( $I_{ss}$ ) Kv currents in adult mouse LVA myocytes in a dose-dependent

manner. Outward  $K_v$  currents were recorded as described in the legend to Figure 4 in the presence and absence of varying concentrations of DPO-1. In each cell, the amplitudes of the individual  $K_v$  current components ( $I_{to,f}$ ,  $I_{K_{slow}}$  and  $I_{ss}$ ) were determined (see Materials and Methods), normalized to the maximal current amplitude in the same cell at each DPO-1 concentration; mean  $\pm$ SEM normalized values for  $I_{to,f}$ ,  $I_{K_{slow}}$  and  $I_{ss}$  are plotted as a function of DPO-1 concentration. (D) Representative single contraction record obtained from an adult WT LVA myocyte in the presence of 100 nM DPO-1 during superfusion with control Tyrode solution containing 100 nM DPO-1 alone or 100 nM DPO-1 plus palmitate:BSA (30  $\mu$ M:60  $\mu$ M). In the presence of 100 nM DPO-1, the mean  $\pm$  SEM decrease in fractional shortening produced by palmitate:BSA was reduced significantly (\*\* $P < 0.01$ ).

Table 1

Effects of Palmitate:BSA(30:60  $\mu$ M) on  $K^+$  Currents in WT, SWAP and Kv2.1<sup>-/-</sup> LVA myocytes<sup>1</sup>

	n	$I_{to,f}$			$I_{K,slow}$		
		$I_{peak}$ (pA/pF)	Density (pA/pF)	$\tau_{decay}$ (ms)	Density (pA/pF)	$\tau_{decay}$ (ms)	$I_{K1}$ (pA/pF)
<b>WT</b>							
Control	24	54 ± 2	32 ± 1	50 ± 2	16 ± 1	1004 ± 45	21 ± 2
Palmitate:BSA		65 ± 2 <sup>***</sup>	35 ± 2 <sup>***</sup>	53 ± 2	22 ± 1 <sup>**</sup>	1011 ± 28	22 ± 2
<b>SWAP</b>							
Control	17	51 ± 3	34 ± 3	47 ± 2	12 ± 1 <sup>+++</sup>	1049 ± 31	--
Palmitate:BSA		58 ± 3 <sup>**</sup>	38 ± 3 <sup>**</sup>	47 ± 2	14 ± 1 <sup>**</sup>	1118 ± 33	--
<b>Kv2.1<sup>-/-</sup></b>							
Control	12	50 ± 3	36 ± 2	40 ± 2 <sup>++</sup>	10 ± 1 <sup>+++</sup>	762 ± 33 <sup>++</sup>	--
Palmitate:BSA		55 ± 3 <sup>**</sup>	38 ± 2 <sup>*</sup>	38 ± 1	12 ± 1 <sup>**</sup>	632 ± 24	--

<sup>1</sup> Currents were evoked at +40 mV from holding potential of -70 mV.\*<sup>\*\*\*</sup>, Values in the presence of palmitate:BSA are significantly (<sup>\*</sup> $P < 0.05$ , <sup>\*\*</sup> $P < 0.01$ , <sup>\*\*\*</sup> $P < 0.001$ ) larger than controls.+, ++, Values are significantly (<sup>+</sup> $P < 0.05$ , <sup>++</sup> $P < 0.01$ ) smaller than in WT LVA cells.